COMPUTER SIMULATION TO PREDICT THE SLIDING WEAR OF PEARLITIC RAILS IN CONTACT BETWEEN CAST AND FORGED RAILWAY WHEELS

JOÃO V.R. SILVA E SILVA[1], LUIZ F.V. CORRÊA[1], RUBSON M. CAMPOREZ[2], CHERLIO SCANDIAN[2] & GUILHERME F. M. DOS SANTOS[1]
[1]Tribology and Railway Dynamics Laboratory, Federal University of Espírito Santo, Brazil
[2]Tribology, Corrosion and Materials Laboratory, Federal University of Espírito Santo, Brazil

ABSTRACT
This work aims to implement and evaluate the effectiveness of the semi-analytical computational method global incremental wear model (GIWM) in predicting the sliding wear of rails in contact with the flange of railway wheels during curves, which is a parameter of great importance for the efficiency of railway operation. The method validation was performed by comparing the wear depth calculated using the GIWM algorithm to the experimental results published in previous work. The data was obtained in dry (relative humidity: 55% ± 10%) pin-on-disc tests carried out on a universal PLINT TE67 tribometer under a normal load of 24.6 N, representing 1.5 GPa of contact pressure. The specimens, hemispherical pins, were extracted from a pearlitic steel rail and the discs were extracted from two different, forged and cast, Class C railway wheels. The tangential sliding speeds were 0.1 m/s and 0.9 m/s, the latter being the most representative according to the literature. The wear model was based on Archard's law for sliding wear and the algorithm was implemented in Python. The results showed good agreement of the wear depth values between the computational and experimental methods for the cast wheel material under higher sliding speed, partial agreement for both wheel materials at lower speed and inconsistency for the forged wheel material under higher sliding speed. Furthermore, the algorithm is computationally efficient, presenting simulation time up to 180 times less than the finite element methods reported in the literature. Therefore, it was concluded that the GIWM method has potential for application in the freight railway sector, which uses cast wheels extensively, to guide technical areas regarding the wear behavior of rails under sliding contact during curves.
Keywords: tribology, railway, sliding wear, Archard, computer simulation, GIWM.

1 INTRODUCTION

Heavy-haul railways development is highly associated with economic growth since it increases transportation efficiency of raw materials [1]. Besides, according to the National Association of Rail Carriers [2], railway cargo transport is responsible for 21.5% of the Brazilian national transportation matrix and there is still plenty of space to grow, indicating the importance in destinate efforts on railway improvement.

However, rail transport operation is subject to wear, especially in the vehicle and rail contact. Miranda et al. [3] emphasizes the relationship between the efficient management of such contact and lowering maintenance costs of rolling and track components. Thus, modelling and predicting the wear mechanisms present in this system is crucial to improve railway operation efficiency.

The wheel–rail contact is the core of scientific researches in respect to the vehicle–track interaction. According to Lewis and Olofsson [4], this contact assumes three basic configurations, as shown in Fig. 1. Region A illustrates the wheel tread–rail head contact that occurs in straight tracks. Further, Region B delineates the wheel flange–rail gauge corner contact that takes place in curved track, exhibiting a large sliding component on the contact patch. Finally, Region C, the most improbable, represents the contact between field sides of

WIT Transactions on The Built Environment, Vol 213, © 2022 WIT Press
www.witpress.com, ISSN 1743-3509 (on-line)
doi:10.2495/CR220081

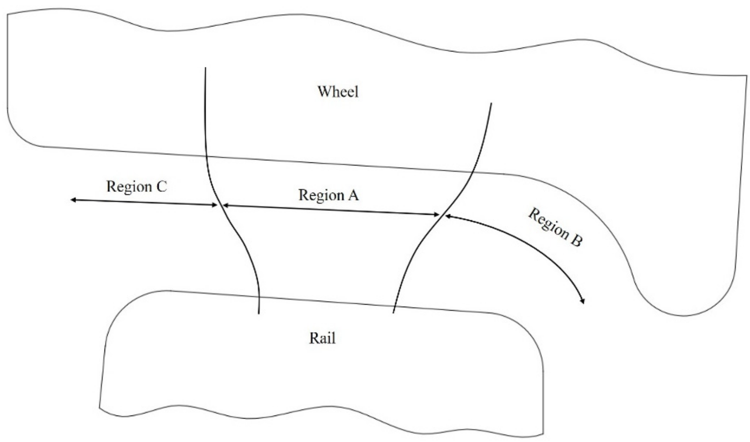

Figure 1: Wheel–rail contact zones. *(Source: Adapted from [4].)*

wheel and rail. In this work, the B case will be scrutinized in view of the fact that this contact condition has a higher potential to cause severe wear compared to the other two [5].

Provided that the appropriate conditions are applied and controlled, laboratory tests may be used to investigate wear mechanisms. The pin-to-disc geometry correctly reproduces the sliding conditions. Furthermore, the nature of the contact is asymmetrical, which means that the pin experiences a continuum contact while the disc experiences an intermittent contact [6].

Hence, this experimental method is extensively employed [7]–[9] to study wear in the contact between the wheel flange, characterized by the disc, and the corner of the track head gauge, characterized by the pin.

Nonetheless, to carry laboratory tests may be onerous and time-consuming resulting in considerable delays in the scientific investigations. Thereupon, simulation tools are interesting solutions for predicting wear. Several researches [11]–[13] were executed to investigate the application of finite element method (FEM) in emulating laboratory tests response.

However, Bastola et al. [11] has shown the necessary precondition of results extrapolation in order to obtain sufficiently accurate results as a consequence of the exorbitant computational time required in the FEM method. Development of more efficient and less time-consuming methods are therefore required.

Regarding sliding wear, Bortoleto et al. [14] cite that several formulations have been investigated in order to describe the different mechanisms involved in this phenomenon. In the 1950s, Archard [15] demonstrated his sliding wear model which according to Liu et al. [16] is widely employed to measure the worn volume as well as the wear depth of body and counter body of the system.

Based on Archard's wear law, Hegadekatte et al. [17] coined a simulation tool named global incremental wear model (GIWM). It is a computationally inexpensive algorithm for predicting pin wear depth or disc wear depth in pin-on-disc tests. This method uses global quantities and updates the contact geometry at each sliding interval with the aim to efficiently determine wear depth. Therefore, the aim of this work is to examine the applicability of the GIWM in efficiently predicting wheel flange–rail gauge corner contact wear depths prevalent in curved tracks and guide engineering decisions.

2 MATERIALS AND METHODS

2.1 Materials

Rail and rail wheel were used to manufacture the pin and disc samples (Fig. 2), respectively. The rail wheels are produced in cast and forged steel class C following the standard of the Association of American Railroads (AAR) and, the rail is conventional pearlitic steel used in railways. The chemical composition of the pins and discs are shown in Table 1 [7].

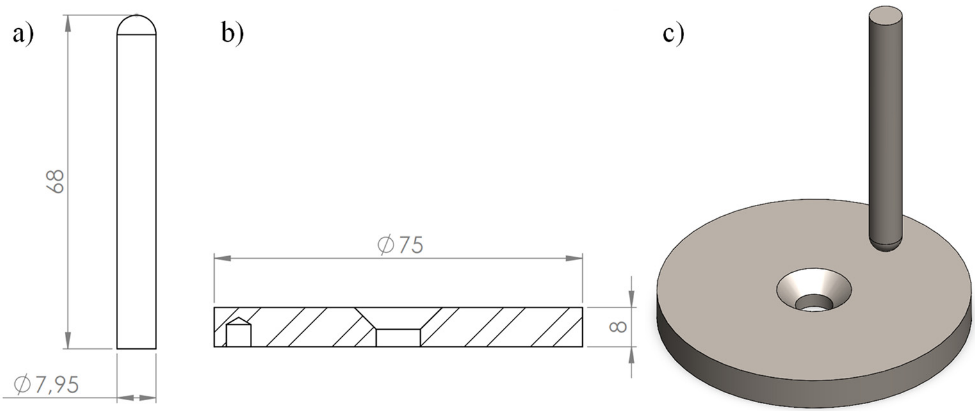

Figure 2: Dimensional, in millimeters, of (a) Pin; and (b) Disc samples; and (c) Schematic assembly. *(Source: Adapted from [7].)*

Table 1: Chemical composition of discs and pins [7].

Materials	C (wt%)	Mn (wt%)	Si (wt%)	P (wt%)	S (wt%)	Cr (wt%)
Pin–Rail	0.72–0.82	0.80–1.25	0.10–0.50	< 0.03	< 0.02	< 0.25
Disc–Wheel	0.67–0.77	0.60–0.90	0.15–1.00	< 0.03	0.005–0.04	–

2.2 Wear tests

Wear tests without lubrication (relative humidity: 55% ± 10%) were performed in pin-on-disc configuration on the PLINT TE67 universal tribometer. For each pair of materials, a normal load of 24.6 N was applied in order to achieve an initial mean contact pressure of 1.5 GPa. The test lasted 1 h and two sliding speeds, 0.1 m/s and 0.9 m/s, were applied. The initial mean contact pressure of 1.5 GPa along with the 0.9 m/s sliding speed constitute the most representative condition for the in the wheel flange–rail gauge corner contact [7].

To this work, only the wear of the pin will be considered, and the results are based on the work by de Almeida et al. [7]. The equations for calculating the wear height (h_p) and consequently the volume (V_p) removed from the pin follow the ASTM G99 standard and will be described ahead in eqns (1) and (2), respectively [18].

$$h_p = R_b - \sqrt{(R_b^2 - r_b^2)}, \tag{1}$$

$$V_p = \frac{\pi h_p}{6}\left(3r_b^2 + h_p^2\right), \quad (2)$$

where: R_b: pin end radius;r_b: wear scar radius.

Specific wear rate, k_p, is calculated from volume loss, V_p, total sliding distance, s_{max}, and normal load, W, applied, eqn (3):

$$k_p = \frac{V_p}{s_{max}W}. \quad (3)$$

In this work, the wear of the pin was evaluated in continuous and interrupted tests. Continuous tests were used to obtain the specific wear rate, and the results of the interrupted tests helped in the comparison with the GIWM model. The wear depth of the pin, interrupted tests, was obtained by eqn (1), the specific wear rate was calculated from the combination of eqns (1), (2) and (3).

2.3 Global incremental wear model (GIWM) for pin-on-disc tests

The term "global" indicates that global quantities are used in the model, i.e., nominal quantities, e.g., average contact pressure or nominal contact pressure, not considering the real contact pressure and in this model, the contact area considers the contribution of elastic deformation and wear, from the pin, orthogonal to the contact surface.

The term "incremental" means that at each step, within the algorithm, variables such as the contact area are being updated, as with each iteration of a predetermined slipped distance, wear changes it and therefore the contact pressure varies, and this will influence the next wear depth [17].

2.3.1 GIWM for wear pin

It is known that the pin and the disc wear out simultaneously during sliding, but for the computer modeling it will be assumed that the disc wear is negligible and that practically all the wear occurs on the pin [17], [19].

To obtain the wear depth of the pin along the slid distance, it is necessary to use the iterative computational model presented in Fig. 3(a), where p is the contact pressure, W is the normal load, a is the radius of contact from elastic deformation and wear, h is the total displacement of the hemispherical tip of the pin, R_p is the radius of the pin, h^e is the deformation elastic, h^w is the wear depth, k_p is the dimensional wear coefficient, Δs is the distance increment, s_{max} is the maximum slip distance, and E_c is the combined modulus of elasticity [6]. The implementation of this computational model was carried out in Python, a high-level, scientific, free, and open-source programming language.

The combined modulus of elasticity, E_c, and the initial contact radius, a_0, are calculated from eqns (4) and (5), respectively [6]:

$$E_c = \left(\frac{1-\nu_p^2}{E_p} + \frac{1-\nu_d^2}{E_d}\right)^{-1}, \quad (4)$$

$$a_0 = \left(\frac{3WR_p}{4E_c}\right)^{\frac{1}{3}}, \quad (5)$$

where: ν_p: Pin Poisson's ratio; ν_d: Disc Poisson's ratio; E_p: Pin elastic modulus; E_d: Disc elastic modulus.

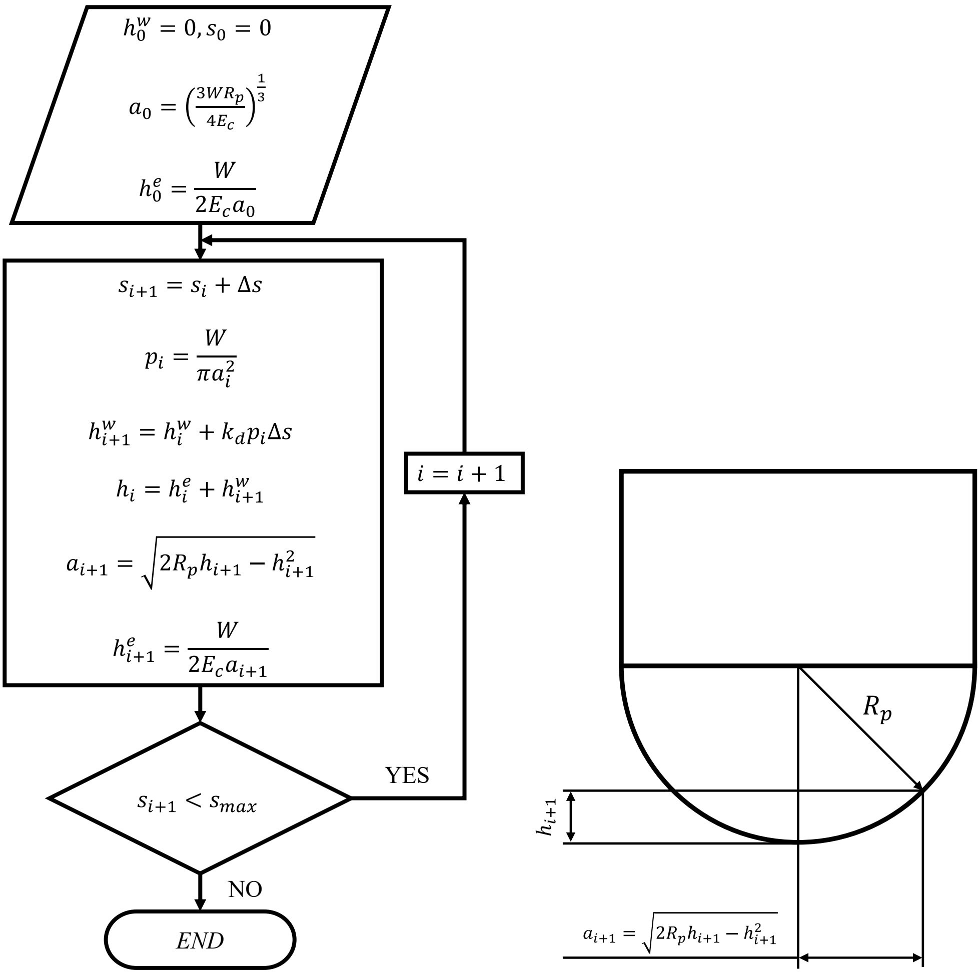

Figure 3: (a) Flow chart of GIWM for pin; and (b) Schematic drawing of the contact radius each Δs and with the combination of elastic deformation and pin wear [17], [19].

The elastic deformation orthogonal to the surface is obtained through eqn (6) [10]:

$$h^e = \frac{W}{2E_c a}. \tag{6}$$

The update of the contact radius, a_i, with each increment of the slipped distance, Δs, is obtained by the sum of the elastic deformation and the wear depth from the contact geometry (Fig. 3(b)) and the wear depth is calculated with Euler explicit model integrated over sliding distance on eqn (7) till the end of the algorithm [17], [19].

$$h_{i+1}^w = k_d p_i \Delta s_i + h_i^w. \tag{7}$$

3 RESULTS AND DISCUSSIONS

Fig. 4(a) and (b) show the comparative results of the semi-analytical GIWM computational simulation with the experimental results found in de Almeida et al. [7], for pearlitic steel pin sliding against forged steel disc with a microstructure of colonies of pearlite interspersed with bainite, under velocities of 0.1 m/s and 0.9 m/s, respectively.

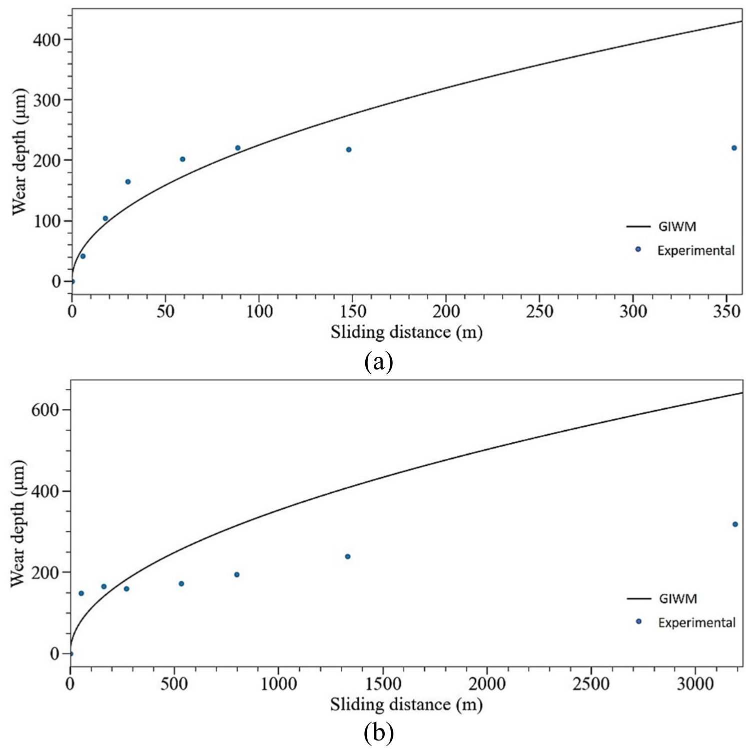

Figure 4: GIWM computer simulation results compared with pin-on-disc tribometer experimental results from de Almeida et al. [7] for the normal load of 24.6 N. (a) Forged steel wheel under sliding speed of 0.1 m/s; and (b) Forged steel wheel under sliding speed of 0.9 m/s.

It can be noted that the semi-analytical method has good agreement with the experimental method until approximately 90 m of sliding distance (running-in), in the case of the lowest sliding speed (Fig. 4(a)). However, after this distance, the GIWM method has low assertiveness.

According to the experimental study under which this paper was based, particles removed from the disc surfaces were highly deformed and had a considerable specific surface area which, according to the researchers, is convenient for the occurrence of rapid oxidation.

The oxidized particles in turn adhere to the disc surface, exponentiated by debris formation, and can cause micro abrasive events on the pin, changing the wear mechanism seen before [7].

It is likely, then, that the GIWM method did not work well from a certain sliding distance, as it does not have the ability to work under a possible oxidative episode that occurred after initiating the experimental test.

For the case of the highest sliding speed (Fig. 4(b)), it can be seen that the semi-analytical method has good agreement with the experimental method only between 100 m and 300 m sliding distance (running-in). After this range, the GIWM method does not work well to simulate the wear of the pearlitic rail.

The result of the computer simulation corroborates the literature and the simulation for cast wheels itself, with regard to the formation of debris and the consequent favoring of the modification of the wear mechanism to oxidative.

Similarly, Fig. 5(a) and (b) show the comparative results of the semi-analytical GIWM computational simulation with the experimental results found in de Almeida et al. [7], for pearlitic steel pin sliding against predominantly pearlitic cast steel disc, under velocities of 0.1 m/s and 0.9 m/s, respectively.

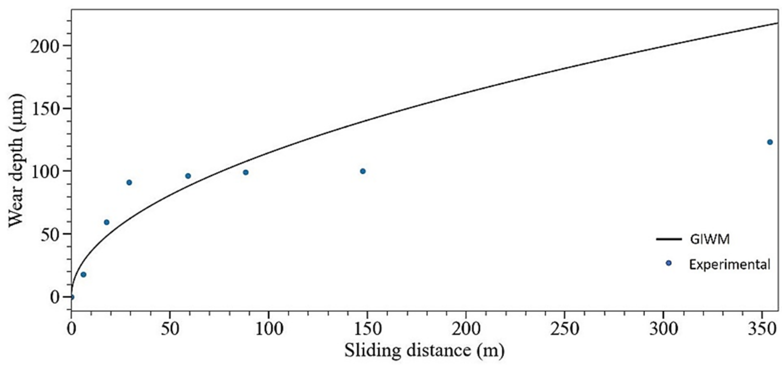

(a)

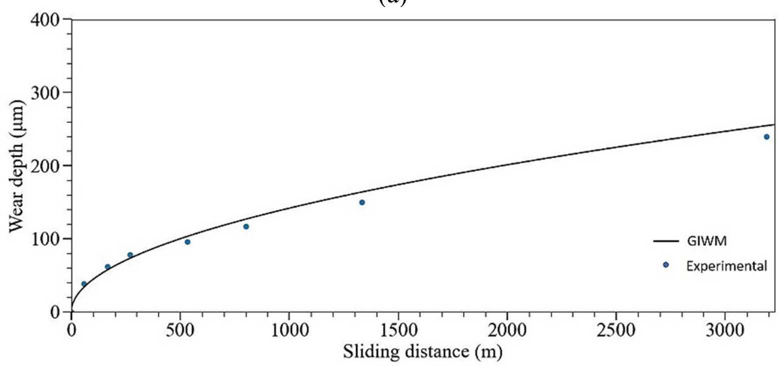

(b)

Figure 5: GIWM computer simulation results compared with pin-on-disc tribometer experimental results from de Almeida et al. [7] for the normal load of 24.6 N. (a) Cast steel wheel under sliding speed of 0.1 m/s; and (b) Cast steel wheel under sliding speed of 0.9 m/s.

In Fig. 5(a), where the sliding condition was tested under speed of 0.1 m/s, a consonance of GIWM result with the same condition for forged wheels is observed, where the method proved assertive only in initial ranges of sliding distances.

A possible reason for the low assertiveness of the method is the high adhesion and plastic deformation observed by de Almeida et al. [7] since the method is based on the stiffness of the materials under unloading conditions and thus the GIWM does not have the ability to act predictively in plastic regime [17], [19]. In addition, de Almeida et al. [7] observed that when the plastic limit was reached, the wear mechanism changed from adhesion to fatigue, which might be another possible reason for the low assertiveness of the method in these cases.

For the case of the higher sliding speed (Fig. 5(b)), it is possible to note a good assertiveness of the GIWM method in the whole extension of the test both in running-in and steady state in comparison with the experiments performed by de Almeida et al. [7].

Probably, the method adapted better due to a lower amount of material adhesion on the pins under this sliding condition, as stated by the researchers. Therefore, a better agreement of the GIWM with laboratory experiments is perceived when the actual conditions of the pair of materials do not favors a change in the wear mechanism involved, as it was said that it occurred for the other three cases tested. Evidence that helps to corroborate this theory can be found in Kurzenhäuser et al. [20].

For all cases tested, simulations via GIWM were considerably faster than analogous simulations via FEM reported in the literature. Bastola et al. [11], for example, performed analyses in their recent work that demanded 12 hours of simulation to reach 0.2% of the total sliding distance. The GIWM simulations of the present work were up to 180 times faster, due to its semi-analytical method of easy computational iteration.

4 CONCLUSIONS

The work in question proposed to evaluate the assertiveness of the semi-analytical method global incremental wear model (GIWM) in predicting the wear behavior of railway tracks, when in curved contact with cast and forged wheels.

The method is based on the incremental calculation of the evolution of the body's worn height through the contact area with the counter-body. The results of the algorithm were compared with results of sliding experiments in the pin–disc configuration present in the literature, where the pin was made with rail sample (body) and the discs with wheel sample (counter–body).

The analysis showed that the GIWM can predict satisfactorily, quickly and cheaply the wear behavior in the running-in period. This is a surprising result because the method was not designed to be sensitive to the switch from running-in to steady state.

However, at steady state the GIWM exhibit erroneous wear predictions in three of the four tests. The only exception was the last case, which represents real operating conditions. Possible reason for that is the abrupt changes in the wear mechanisms involved observed in those tribosystems, since this method only works when the active wear mechanism remains the same [20]. Future investigations on interrupted tests shall be taken in order to inspect the wear mechanism change and inspect the correlation between it and the method's accuracy.

All tests with GIWM were exorbitantly more computationally efficient than similar simulations in FEM listed in the literature, in addition to having very equivalent responses between them [21]. This fact shows that the semi-analytical method has the potential to quickly orient the railway sector in constant relation to the materials and the dynamics of use it has already known and constant use.

ACKNOWLEDGEMENT
The authors are grateful for the support of Vale S.A. (Cátedra de Vagões Program).

REFERENCES

[1] Bai, W., Zhou, L., Wang, P., Hu, Y., Wang, W., Ding, H., Han, Z., Xu, X. & Zhu, M., Damage behavior of heavy-haul rail steels used from the mild conditions to harsh conditions. *Wear*, **496–497**, 204290, 2022.
[2] ANTF, National Association of Railway Carriers, General information. Brasilia, Brazil, 2022. www.antf.org.br/informacoes-gerais/. Accessed on: 31 Jul. 2022.
[3] Miranda, R.S., Rezende, A.B., Fonseca, S.T., Fernandes, F.M., Sinatora, A. & Mei, P.R., Fatigue and wear behavior of pearlitic and bainitic microstructures with the same chemical composition and hardness using twin-disc tests. *Wear*, **494–495**, 2022.
[4] Lewis, R. & Olofsson, U., Basic tribology of the wheel–rail contact. *Wheel–Rail Interface Handbook*, 1st ed., pp. 34–57, 2009.
[5] Lewis, R. & Olofsson, U., Mapping rail wear regimes and transitions. *Wear*, **257**, pp. 721–729, 2004.
[6] Hutchings, I. & Shipway, P., *Tribology: Friction and Wear of Engineering Materials*, Butterworth-Heinemann, 2017.
[7] de Almeida, L.P.F., Falqueto, L.E., Goldenstein, H., Bozzi, A.C. & Scandian, C., Study of sliding wear of the wheel flange: Rail gauge corner contact conditions – Comparative between cast and forged steel wheel materials. *Wear*, **432–433**, 2019.
[8] Sundh, J., Olofsson, U. & Sundvall, K., Seizure and wear rate testing of wheel–rail contacts under lubricated conditions using pin-on-disc methodology. *Wear*, **265**, pp. 1425–1430, 2008. DOI: 10.1016/j.wear.2008.03.025.
[9] Danks, D. & Clayton, P., Comparison of the wear process for eutectoid rail steels: Field and laboratory tests. *Wear*, **120**, pp. 233–250, 1987.
[10] Oliver, W.C. & Pharr, G.M., An improved technique for determining hardness and elastic modulus using load and displacement sensing indentation experiments. *J. Mat. Res*., **7**, pp. 1564–1583, 1992.
[11] Bastola, A., Stewart, D. & Dini, D., Three-dimensional finite element simulation and experimental validation of sliding wear. *Wear*, 2022.
[12] Hegadekatte, V., Huber, N. & Kraft, O., Finite element-based simulation of dry sliding wear. *Modelling and Simulation in Materials Science and Engineering*, **13**, pp. 57–75, 2005.
[13] Põdra, P. & Andersson, S., Simulating sliding wear with finite element method. *Tribology International*, **32**, pp. 71–81, 1999.
[14] Bortoleto, E.M., Rovani, A.C., Seriacopi, V., Profito, F.J., Zachariadis, D.C., Machado, I.F., Sinatora, A. & Souza, R.M., Experimental and numerical analysis of dry contact in the pin on disc test. *Wear*, **301**, pp. 19–26, 2013.
[15] Archard, J.F., Contact and rubbing of flat surfaces. *Journal of Applied Physics*, **24**(8), pp. 981–988, 1953.
[16] Liu, B., Bruni, S. & Lewis, R., Numerical calculation of wear in rolling contact based on the Archard equation: Effect of contact parameters and consideration of uncertainties. *Wear*, 2021.
[17] Hegadekatte, V., Huber, N. & Kraft, O., Modeling and simulation of wear in a pin on disc tribometer. *Tribology Letters*, **24**, pp. 51–60, 2006.
[18] ASTM G99, Standard Test Method for Wear Testing with a Pin-On-Disk Apparatus, 2017.

[19] Hegadekatte, V. et al., A predictive modeling scheme for wear in tribometers. *Tribology International*, **41**(11), pp. 1020–1031, 2008.
[20] Kurzenhäuser, S., Hegadekatte, V., Schneider, J., Huber, N., Kraft, O. & Zum Gahr, K.-H., Tribological characterization and numerical wear simulation of microcomponents under sliding and rolling conditions. *Microsyst. Technol.*, **14**, pp. 1839–1846, 2008.
[21] Jamari, J., Wear prediction using GIWM (global incremental wear model) method. *ROTASI*, **11**(4), pp. 1–4, 2012.